

# Phenomenology of metal-semiconductor electrical barriers\*

T. C. McGill

California Institute of Technology, Pasadena, California 91109

(Received 30 August 1974)

The phenomenological rules governing the values of electrical barriers between metals, and semiconductors or insulators are reviewed. The barrier energies on ionic insulators are shown to vary strongly with metal electronegativity, while in the case of covalent semiconductors, the barrier energies are relatively independent of the metal. The barrier energy from the metal Fermi level to the conduction band of the semiconductor is shown to be approximately two thirds of the semiconductor band gap with certain exceptions. The success of a simple barrier model in accounting for the properties of the barrier are reviewed. The variation of barrier energy with electrical field is reported for Al-SiO<sub>2</sub>, Al-GaSe, and Al-GaAs and compared with simple theory including image-force lowering and field penetration into the metal. Transport through interfacial barriers is illustrated by discussing transport through metal-GaSe-metal structures and metal-InAs Schottky barriers.

## I. INTRODUCTION

The study of electrical interface barriers dates back to 1874, when K. F. Braun<sup>1</sup> observed that an interface formed by a metal wire brought into contact with a lead sulfide crystal carried current more easily in one direction than in the other. While this result was rather puzzling at the time, it can be explained by postulating that a certain energy is required to take an electron from the Fermi energy of the metal and place it in the conduction band of the lead sulfide crystal. This energy is called the interfacial barrier energy  $\phi_B$ . Since that first observation, interfacial barriers have been studied extensively by a large number of workers.<sup>2</sup> In this paper we would like to summarize some of the results of these investigations and place them in a form to highlight their importance in theoretical considerations of this phenomenon.

We divide our discussion into three parts. First, we summarize a series of empirical rules which tell how the magnitude of the barrier energy varies as we change the metal on a given insulator or semiconductor, and how large the barrier energies are on a covalent semiconductor. Second, we discuss the variation of the barrier energy with electric field. Finally, we summarize the various modes of current transport across (or through) interfacial barriers.

## II. EMPIRICAL RULES FOR BARRIER ENERGIES

From the study of the size of  $\phi_B$  for a rather large number of semiconductors and insulators, two empirical rules have been noted. The first of these rules deals with the variation of  $\phi_B$  on a given insulator or semiconductor as we change the metal electronegativity. The second deals with the magnitude of  $\phi_B$  for metals on covalent semiconductors.

Let us start with the first of these two rules. Simple considerations of how the barrier forms<sup>3</sup> suggests that  $\phi_B$  should be written as the difference of two quantities: one characteristic of the metal vacuum interface, and the other characteristic of the insulator-vacuum or semiconductor-vacuum interface. The first of these is the work function of the metal  $\phi_W$ , the energy required to take an electron from the Fermi energy of the metal into the vacuum; and the second is the electron affinity of the insulator or semiconductor  $\chi_s$ , the energy gained by taking an electron in vacuum and placing it at the bottom of the conduction band of the semi-

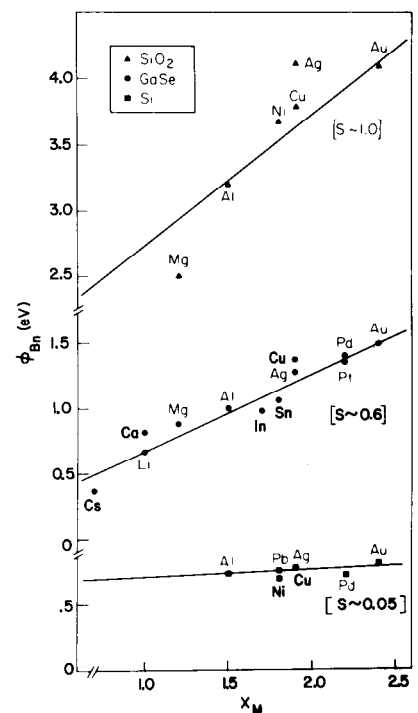


FIG. 1. Barrier energies of various metals on SiO<sub>2</sub>, GaSe, and Si versus the electronegativity  $X_M$  of the metal (after Ref. 7).  $S$  is the slope of the line drawn through the experimental points.

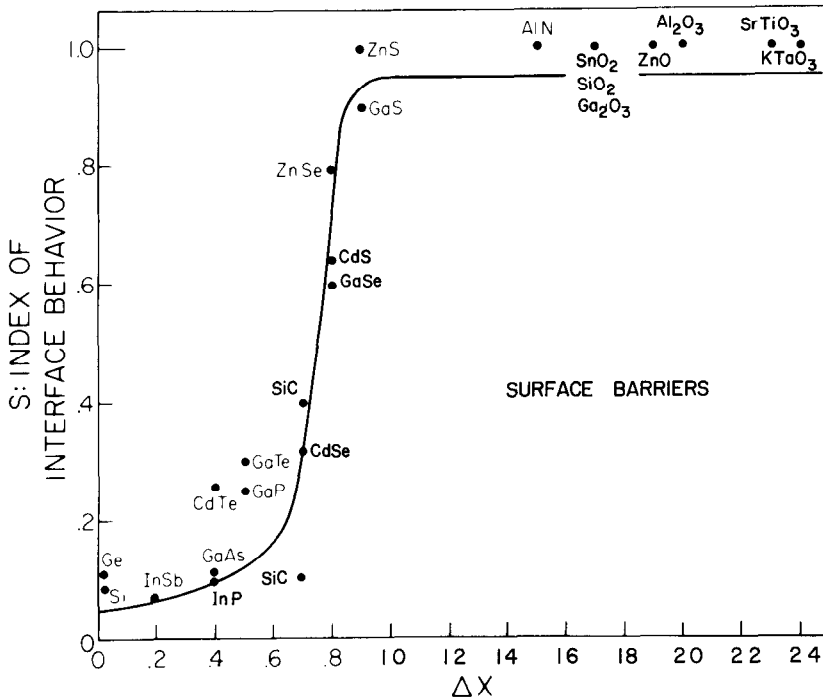


FIG. 2. The slope of the line through the barrier energies as a function of the electronegativity  $X_M$  of the metal versus the electronegativity difference of the insulator or semiconductor (after Ref. 7).

conductor or insulator. That is,

$$\phi_B = \Phi_W - \chi_s \quad (1)$$

The work function characterizes the metal-vacuum interface and is not ideally suited to the metal-solid interface. For this reason and the fact that accurate values of  $\phi_W$ <sup>4</sup> are not readily accessible for all the metals of interest, we will use the electronegativity<sup>5</sup> of the metal  $X_M$ . The values of  $\phi_W$  are closely related to those of  $X_M$  except for a constant. This substitution has no important effect on the results that are to follow.

Hence, we have that

$$\phi_B = X_M - \chi_s + \text{const.} \quad (2)$$

This simple argument would lead us to conclude that the barrier energy should increase linearly as we vary the electronegativity of the metal with a slope of unity. More generally, we might write that

$$\phi_B \cong SX_M + \text{const.}, \quad (3)$$

where  $S$  is the slope of the variation of the barrier energy

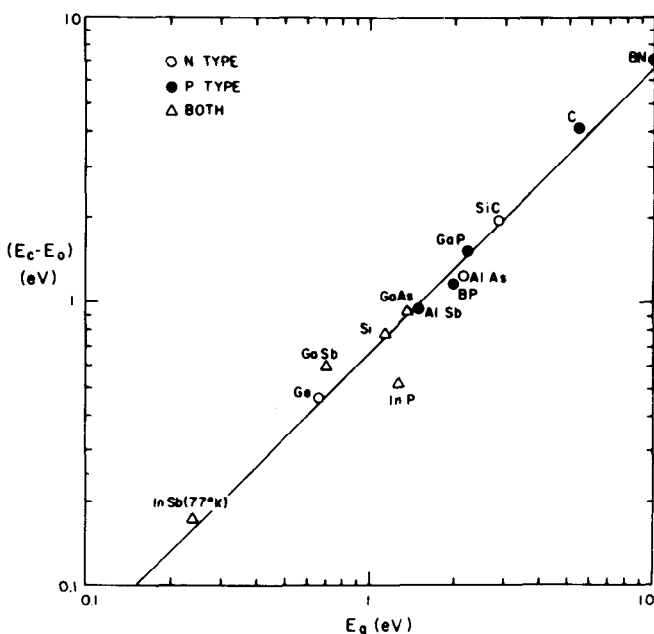


FIG. 3. Barrier energies for zinc-blende materials as a function of the band gap of the semiconductor (after Ref. 14).

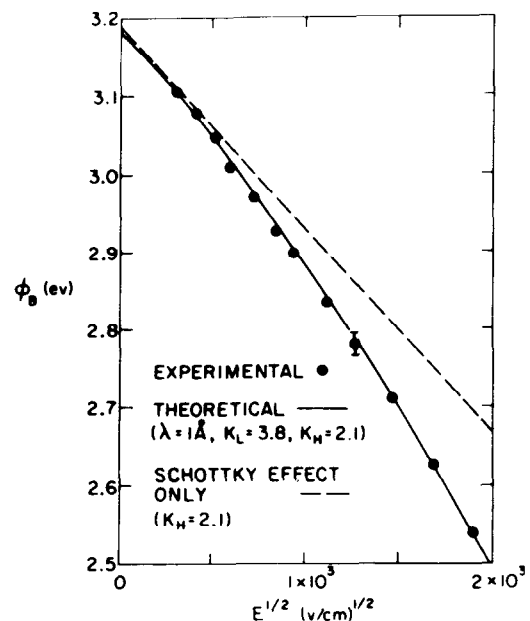


FIG. 4. Al-SiO<sub>2</sub> barrier energy as a function of the square root of the electric field in the SiO<sub>2</sub> (after Ref. 16). The dashed curve is given by the first and second term in Eq. (5). The solid curve includes all the terms in Eq. (5).

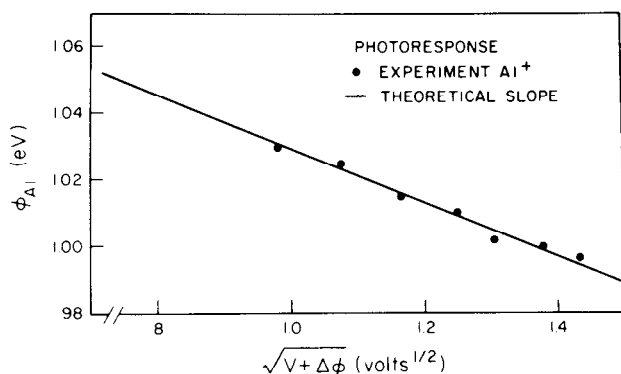


FIG. 5. Al-GaSe barrier energy as a function of the square root of the applied bias (after Ref. 17). The solid curve is the values obtained from Eq. (5).

with the electronegativity of the metal. The simple theory would suggest that  $S$  should be unity.

In Fig. 1, we have plotted the values of  $\phi_B$  vs  $X_M$  for three different insulators or semiconductors  $\text{SiO}_2$ , GaSe, and Si. In the case of  $\text{SiO}_2$ , the slope  $S$  is approximately one. While in the case of GaSe, it is 0.6; and in the case of Si, it is approximately zero. This shows that the values of  $S$  can be quite different from the simple theory; and, since  $\text{SiO}_2$  is more ionic than GaSe which in turn is more ionic than Si, it suggests that the value of  $S$  depends upon the ionicity of the semiconductor or insulator. To illustrate this point further, we take as a measure of the ionicity of an AB compound<sup>5,6</sup> the difference in the electronegativities of the two constituents

$$\Delta X = X_B - X_A, \quad (4)$$

where  $X_A$  is the electronegativity of the species A and  $X_B$  is the electronegativity of the species B. Then if we plot  $S$  vs  $\Delta X$ , we obtain the rather surprising results shown in Fig. 2.<sup>7</sup> The value of  $S$  is quantitatively determined by  $\Delta X$  with  $S$  remaining small for  $\Delta X < 0.7$  and then changing rather rapidly to a value of  $S$  equal to unity for  $\Delta X > 0.7$ . That is, for ionic materials where  $\Delta X > 0.7$ ,  $\phi_B$  varies directly with the electronegativity of the metal. While for  $\Delta X < 0.7$ ,  $\phi_B$  depends rather weakly on the electronegativity of the metal.

Since the behavior of the more ionic materials can be understood qualitatively in terms of the simple ideas mentioned above, most theoretical effort<sup>8-13</sup> has been concentrated upon accounting for the behavior of the more covalent materials and explaining why an abrupt transition in behavior should occur when  $\Delta X \approx 0.7$ .

The second empirical rule for barriers deals with the magnitude of the barrier energy of a metal on covalent semiconductors. If one studies the size of  $\phi_B$  for the covalent semiconductors, one finds with a few exceptions that the barrier energy is at approximately  $\frac{2}{3}$  the band gap  $E_g$ .<sup>14</sup> To illustrate this point, Mead and Spitzer have plotted the barrier energy of Au on a number of different covalent semiconductors as a function of the band gap of the semiconductor in Fig. 3. The straight line in the figure is the line  $\phi_B = 2E_g/3$ .

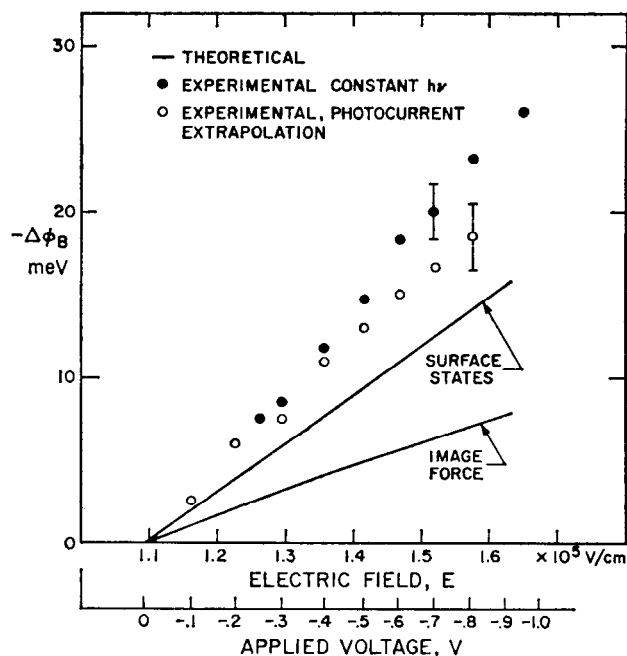


FIG. 6. The change in the Al-GaAs barrier energy as a function of the electric field at the interface (after Ref. 18). The two methods of experimentally determining the barrier energy are discussed in Ref. 18. The curve labeled image force is that obtained from Eq. (5). The curve labeled surface states includes an exponential charge density in the GaAs as discussed in Ref. 18.

In summary, the barrier energy varies according to Eq (2) for metals on ionic materials and is relatively independent of the metal for metals on covalent semiconductors. For metals on covalent semiconductors, the barrier energy is approximately  $\frac{2}{3}$  of the band gap.

### III. VARIATION OF BARRIER ENERGY WITH ELECTRIC FIELD

When an electric field is applied to the metal-insulator structure, we might expect that the electrical barrier would be dependent upon the size of the electric field. The simplest theory includes the image force potential of an electron in the insulator and the field penetration

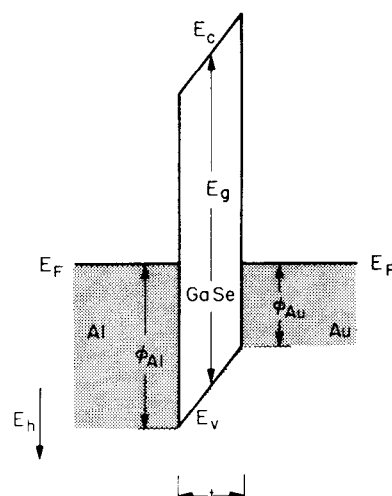


FIG. 7. Energy band diagram of an Al-GaSe-Au structure under zero applied bias (after Ref. 17). Hole energy increases downward.  $E_g$  is the bandgap of GaSe, 2.0 eV.  $\phi_{Al}$  is the Al-GaSe barrier energy, 1.05 eV.  $\phi_{Au}$  is the Au-GaSe barrier energy, 0.52 eV.  $E_F$  is the Fermi level.

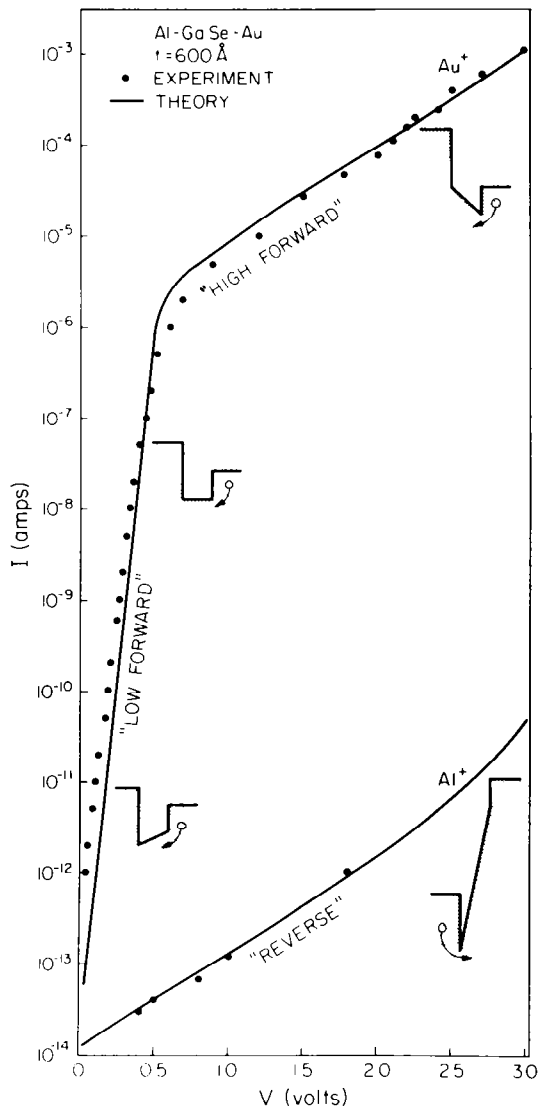


FIG. 8. Current-voltage characteristic of an Al-GaSe-Au structure (after Ref. 17). The dots are experimental data; the solid line is calculated as described in Ref. 15. The insets show the partial band diagram of the Al-GaSe-Au structure and illustrate the various bias conditions.

into the metal.<sup>15</sup> This theory gives

$$\phi = \phi_0 - \left( \frac{qE}{4\pi\epsilon_4 K_H} \right)^{\frac{1}{2}} - K_L \lambda E, \quad (5)$$

where  $\phi_0$  is the zero field barrier energy;  $K_H$  and  $K_L$  are the high- and low-field dielectric constants, respectively; and  $\lambda$  is the Thomas-Fermi screening distance in the metal. While there is not a lot of data available on the field dependence of the barrier, there have been measurements on Al-SiO<sub>2</sub> (ionic),<sup>16</sup> Al-GaSe (intermediate),<sup>17</sup> and Al-GaAs (covalent).<sup>18</sup>

The data on Al-SiO<sub>2</sub> (Fig. 4), and that on Al-GaSe (Fig. 5) are in good agreement with Eq. (5). The data on Al-GaAs (Fig. 6) is in definite disagreement with Eq. (5). Better agreement can be obtained by postulating a charge distribution in the GaAs which is exponentially damped away from the Al-GaAs interface. This charge distribution is attributed to occupied

interface states. While the data are incomplete in that only a few materials have been measured, and the experiments are rather difficult to perform and are subject to a number of unknowns such as dopant charge distribution in the semiconductors, these results do suggest that there is a correlation between deviation from Eq. (5) and the covalency of the material.

#### IV. ELECTRICAL TRANSPORT OVER AND THROUGH INTERFACIAL BARRIERS

The electrical barrier at the interface between a metal and an insulator or semiconductor can be explored experimentally by studying the transport of current through the interface. This can be accomplished in two ways: First by exciting electrons over the barrier using light and studying the photocurrent,<sup>2</sup> and second measuring the current transport due to electrons which are thermally excited over the barrier<sup>17</sup> or due to electrons which tunnel through the barrier.<sup>19-22</sup> In this paper we concentrate upon the second of these two methods.

One of the simplest ways of studying the influence the interfacial barrier on current transport is to make samples in which the current transport is limited by the interfacial barrier. One such structure consisting of Al, a thin layer of GaSe, and Au is shown in Fig. 7. In this case the barrier energies are measured from the Fermi level of the metal to the valence band of the GaSe. The values of the various parameters relevant to GaSe are given in Ref. 17.

If the thickness of the GaSe layer is greater than a few hundred Ångströms, then the current is carried by carriers which are thermally excited over the barrier. Hence the current should vary as the number of carriers which have a thermal energy large enough to surmount the barrier. That is,

$$J \approx J_0 \exp(-\phi_{\text{eff}}/k_B T), \quad (6)$$

where  $\phi_{\text{eff}}$  is the barrier height limiting the current flow. Current-voltage characteristics,  $I$ - $V$ , like those given by Eq. (6) are observed in Au-GaSe-Al struc-

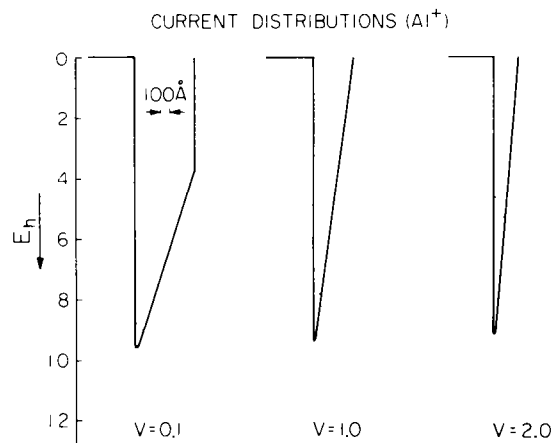


FIG. 9. Theoretical (normalized) current distributions for a reverse biased 600 Å thick Al-GaSe-Au structure (after Ref. 17). The solid curves illustrate the shape of the image-lowered potential barrier; the dotted curves represent the distribution, as a function of hole energy  $E$ , of the injected carriers.

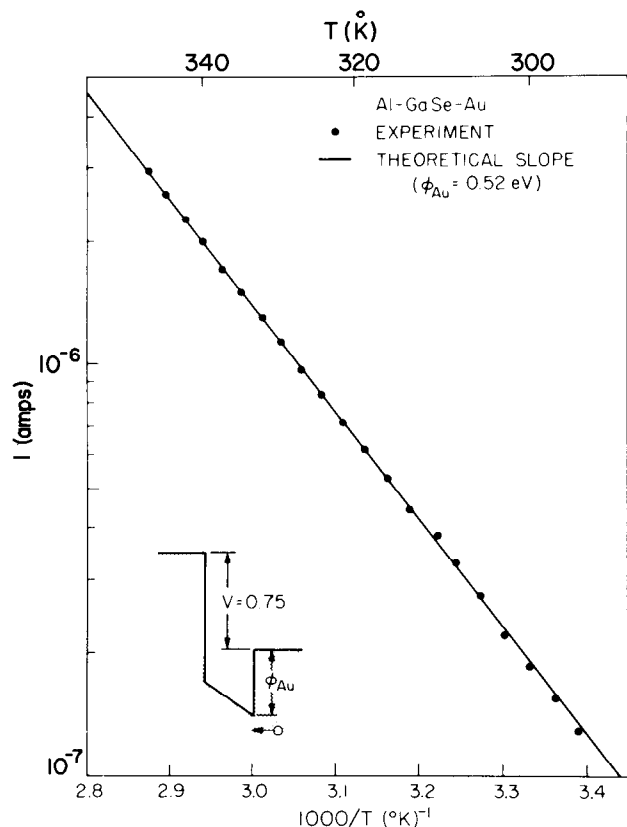


FIG. 10. Current as a function of  $1000/T$  for the Au electrode buried +0.75 Volts on a 600 Å-thick Al-GaSe-Au structure (after Ref. 17). The dots are experimental data; the solid line is calculated as described in Ref. 15.

tures as shown in Fig. 8. In the "low forward" the current flow of holes from the Au is limited by the Al-GaSe barrier which is reduced in value with respect to the Fermi level of Au. In the "high forward" the current flow of holes from the Au is limited by the Au-GaSe

barrier which in the first approximation does not move with respect to the Fermi level of the Au. However, once the image in the metal of the carrier in the insulator is included in the calculation of the barrier shape, the barrier becomes field dependent and lowers slightly with increasing bias.<sup>17</sup> This leads to the observed increase of current with voltage.

In the "reverse direction" the current is due to holes from the Al and is limited by the Al-GaSe barrier. As in the case of the "high forward" the barrier height should vary slowly with bias due to the image lowering of the barrier. However, the current increases more sharply than predicted by the simple-image lowering. The rather large rate of increase of the current with applied bias is due to the fact that the barrier can become so sharply peaked at high biases that holes can actually tunnel through the top of the barrier. This phenomenon is illustrated in Fig. 9, where we have plotted the distribution of current due to holes as a function of the hole energy along the barrier shape. As can be seen from this figure, the current at a small bias is carried mainly by carriers coming over the top of the barrier. While at a large bias, the current is due mainly to the electrons which have been thermally excited and then tunneled through the top of the barrier.

One simple experimental verification of the current expression given in Eq. (6) is the temperature dependence of the current. One would expect that the current for fixed voltage should decrease exponentially with  $1/T$  with a slope given by the barrier energy divided by Boltzmann's constant. In Fig. 10 we have the results of measuring the temperature dependence of the current when the sample is biased in the "high

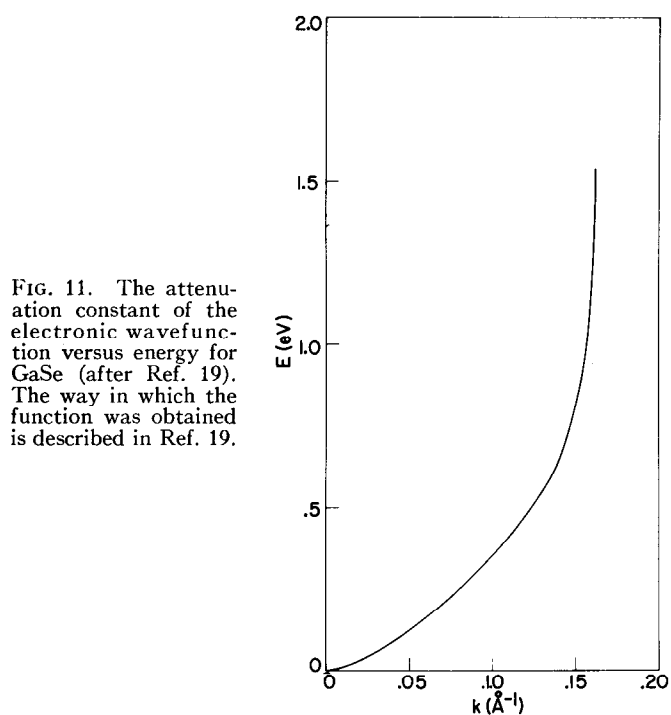


FIG. 11. The attenuation constant of the electronic wavefunction versus energy for GaSe (after Ref. 19). The way in which the function was obtained is described in Ref. 19.

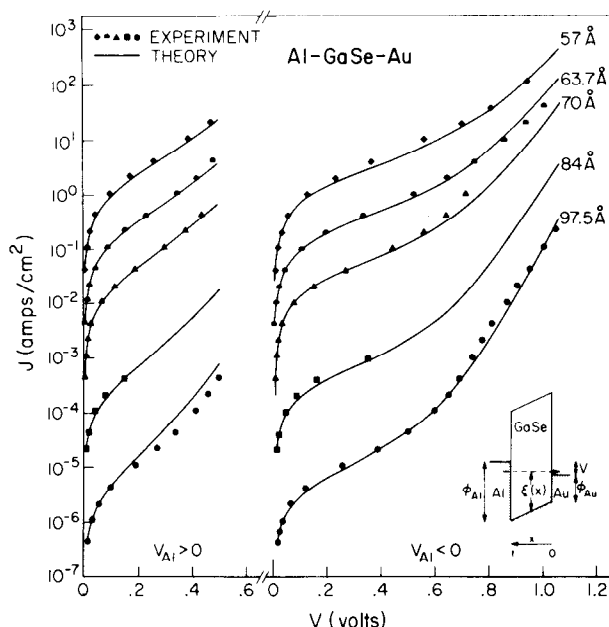


FIG. 12. Current-voltage curves, for both directions of applied bias, of a number of Al-GaSe-Au structures (after Ref. 19). Solid symbols represent experimental data. The solid lines are theoretical curves generated in a manner described in Ref. 19.

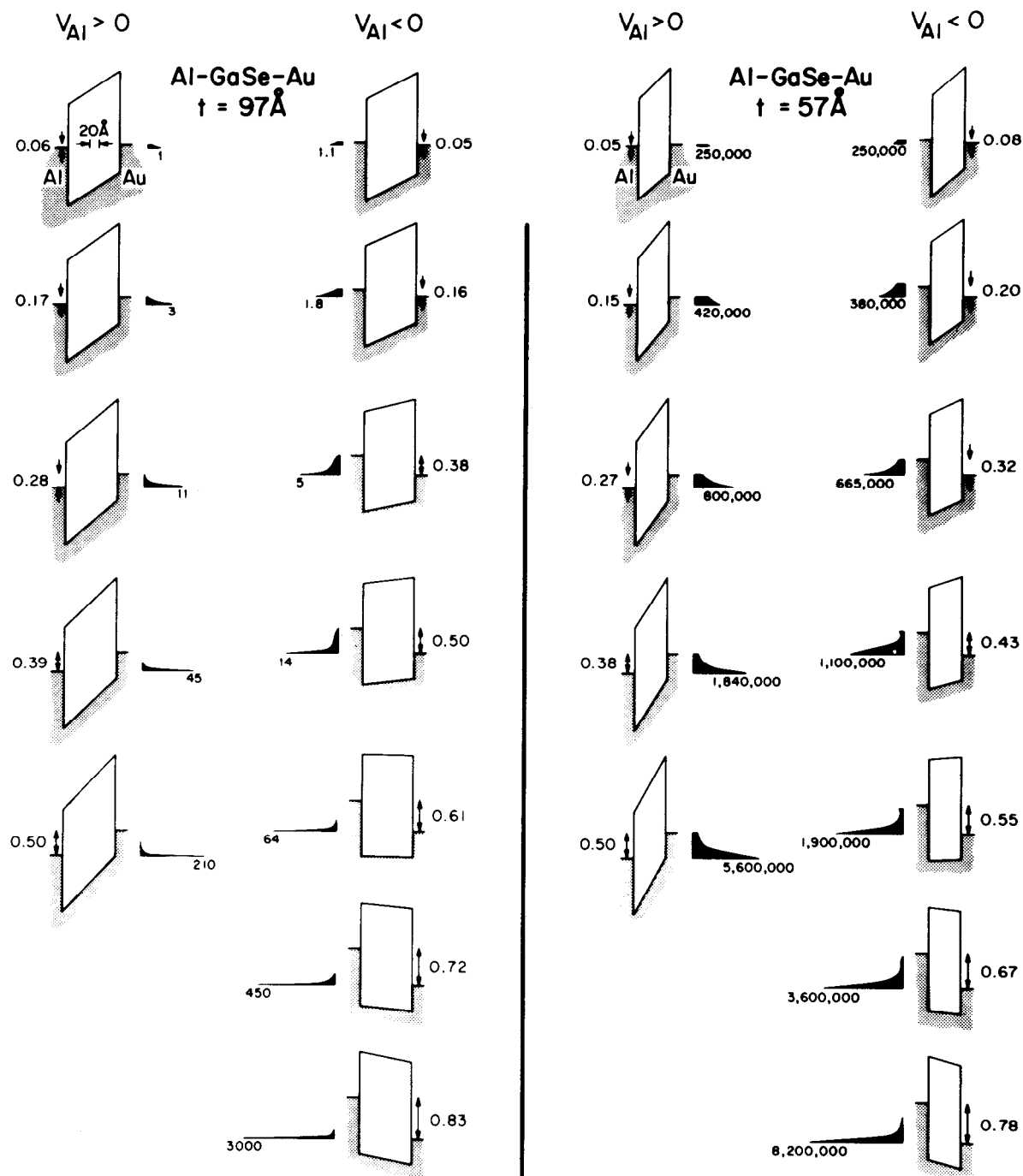


FIG. 13. Energy distributions of tunneling electrons and corresponding band diagrams for two Al-GaSe-Au structures (after Ref. 19). The calculation of these distributions is described in Ref. 19. The number beneath the peak of each distribution indicates the absolute magnitude of the peak relative to the peak of every other distribution in the figure.

forward." The correct exponential activation of the current is observed.

For very thin samples, less than 100 Å, the current-voltage characteristic of the devices is different from those observed for devices with thicker insulators. In this case the current is due to the tunneling of electrons through the insulator. One might expect that the wavefunction of the tunneling electron would be exponentially attenuated as it passes through the insulator. The attenuation would in the simplest case (of relatively small electric field) be dependent upon the energy of the electron relative to the valence band.

Hence, we would expect that the probability of an electron in the metal with a given energy  $E$  tunneling would be given by

$$P(E) = \exp \left[ -2 \int k(\epsilon) dx \right], \quad (7)$$

where  $k(\epsilon)$  is the decay constant for a given energy  $\epsilon$  measured with respect to the valence band or conduction band of the insulator, and the integral is taken over the distance  $x$  in which the electron is in the forbidden gap of the insulator. We can distinguish two cases:

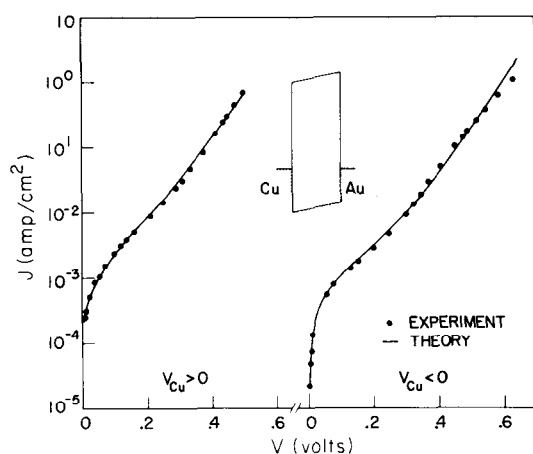


FIG. 14. Experimental current-voltage curve of an 83 Å thick Cu-GaSe-Au structure is shown by the solid symbols (after Ref. 19). The solid curve is the theoretical current-voltage curve described in Ref. 19.

One in which the electron has an energy such that it is in the forbidden gap of the insulator during the entire distance across the insulator, and one in which the electron has an energy such that it is in the forbidden gap of the insulator only during part of the distance across the insulator. We discuss the former case first.

In this case, the total current density  $J$  would be given by the integral over those electrons which are below the Fermi energy of one metal and above the Fermi energy of the other metal.<sup>19</sup> That is

$$J = A \int dE P(E), \quad (8)$$

where  $A$  is approximately constant.<sup>19</sup> In the case of GaSe, all the tunneling characteristics can be explained by using the function  $k(\epsilon)$  given in Fig. 11. (The zero of energy is taken at the valence band edge in this figure.)

Typical experimental current-voltage,  $I$ - $V$ , characteristics as a function of thickness are shown in Fig.

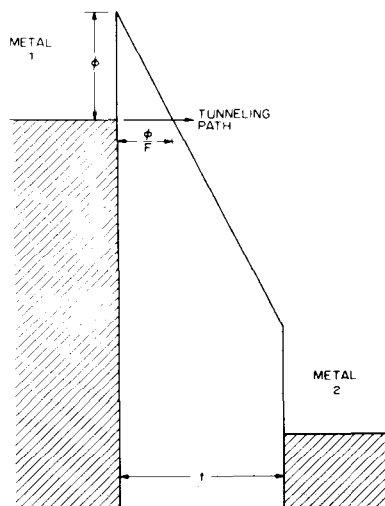


FIG. 15. Energy diagram of a thick metal-insulator-metal structure under high applied bias. Note that the tunneling distance is  $\phi/F$ .

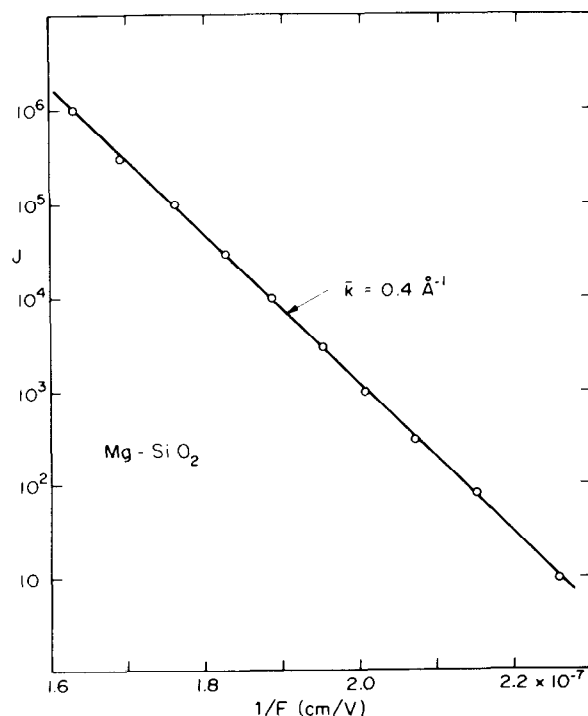


FIG. 16. Fowler-Nordheim plot of the current-voltage characteristics of SiO<sub>2</sub>-Mg (after Ref. 21). The current is normalized such that it is one at the lowest fields.

12. In this figure we have also included the current-voltage characteristic to be expected from an equation similar to Eq. (8).<sup>19</sup> The agreement of the experimental  $I$ - $V$  with the theoretical  $I$ - $V$  for a number of different thicknesses using a single function  $k(\epsilon)$  verifies at least qualitatively that the tunneling model gives a good account of the  $I$ - $V$  characteristics. To give some idea of the dependence of the distribution of tunneling electrons upon the thickness of the insulator, we have plotted the current distribution for a few voltages in Fig. 13. From this figure one can see the big difference in the current distributions for the two different thicknesses. Finally, we consider the result of changing one of the interfaces. That is, we replace the Al by Cu and

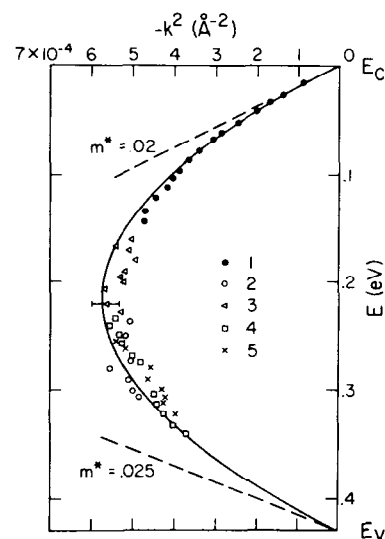


FIG. 17. Attenuation constant versus energy for InAs (after Ref. 22). The solid curve is the two-band expression for  $m^* = 0.02$ . The method for obtaining the various sets of experimental points is discussed in Ref. 22.

measure the  $I$ - $V$  characteristic of an Au-GaSe-Cu structure. The resulting  $I$ - $V$  characteristic is shown in Fig. 14 along with the theoretical  $I$ - $V$  curve computed from Eq. (7). The agreement is quite good.

When the potential applied to the sample is large enough, we have a second type of tunneling called Fowler-Nordheim tunneling.<sup>20</sup> In this mechanism of current flow, an electron near the Fermi energy of the metal tunnels into the insulator and then is transported across the insulator into a second collecting metal (see Fig. 15). In this situation the current is given by the probability that the electron tunnels through the uppermost triangular part of the barrier. The distance that the electron has to tunnel is given by  $\phi/F$ , where  $F$  is the applied field (see Fig. 15). Hence, the current-voltage characteristic should go as

$$J \approx J_0 \exp \left[ \frac{-2\phi\bar{k}}{F} \right], \quad (8)$$

where  $\bar{k}$  is the average decay constant of the wavefunction in the insulator at energies from  $\phi$  to the conduction band. An experimental  $I$ - $V$  characteristic for Mg-SiO<sub>2</sub> interface<sup>21</sup> is given in Fig. 16 where the log of  $J$  is plotted as a function of the reciprocal of the field. The agreement is quite good between theory and experiment.

Finally, one can observe tunneling in Schottky diodes made with fairly heavily doped semiconductors. Parker and Mead<sup>22</sup> have studied this phenomenon in Au-InAs, Cu-InAs, Al-InAs Schottky diodes. In these experiments, they find that the  $I$ - $V$  characteristics are accounted for by assuming that the electronic wavefunction for energies in the forbidden gap is attenuated exponentially with an attenuation constant versus energy as shown in Fig. 17. This attenuation coefficient vs energy is that expected from the bulk band structure of InAs.

## V. SUMMARY

In summary we have reviewed some of the empirical rules governing the barrier energies at metal-semiconductor and metal-insulator contacts and found that there are some striking regularities in the variation and magnitude of the barrier energies. We have also reviewed the change in the barrier energy with field and the various modes of current transport through interfaces and shown that there is quite good qualitative, if not quantitative, agreement of the experimental results with highly simplified model theories of transport through interfaces.

\*Supported in part by the Office of Naval Research under Contract No. N00014-67-A-0094-0036.

<sup>1</sup>K. F. Braun, Ann. Phys. Pogg. **153**, 556 (1874).

<sup>2</sup>See for example, C. A. Mead, Solid State Electro. **9**, 1023 (1966).

<sup>3</sup>See for example, A. Many, Y. Goldstein, and N. B. Grover, *Semiconductor Surfaces* (North-Holland, Amsterdam, 1965), p. 131 ff.

<sup>4</sup>J. C. Riviere (unpublished Report of the Metallurgy Division of Atomic Energy Research Establishment at Harwell, U. K., 1967).

<sup>5</sup>L. Pauling, *The Nature of the Chemical Bond* (Cornell U. P., Ithaca, NY, 1960), 3rd ed., p. 93.

<sup>6</sup>J. C. Phillips, Rev. Mod. Phys. **42**, 317 (1970).

<sup>7</sup>S. Kurtin, T. C. McGill, and C. A. Mead, Phys. Rev. Lett. **22**, 1433 (1969).

<sup>8</sup>J. Bardeen, Phys. Rev. **71**, 717 (1947).

<sup>9</sup>V. Heine, Phys. Rev. **A138** 1689 (1965).

<sup>10</sup>J. C. Phillips, Solid State Comm. **12**, 861 (1973);

<sup>11</sup>J. C. Inkson, J. Phys. C. **6**, 1350 (1973);

<sup>12</sup>B. Pellegrini, Phys. Rev. **B7**, 5299 (1973).

<sup>13</sup>E. Louis and F. Yndurain, Phys. Stat. Sol. **57b**, 175 (1973).

<sup>14</sup>C. A. Mead and W. G. Spitzer, Phys. Rev. **A134**, 713 (1964).

<sup>15</sup>J. G. Simmons, Phys. Lett. **16**, 233 (1965).

<sup>16</sup>C. A. Mead, E. H. Snow, and B. E. Deal, Appl. Phys. Lett. **9**, 53 (1966).

<sup>17</sup>T. C. McGill, S. Kurtin, L. Fishbone, and C. A. Mead, J. Appl. Phys. **41**, 3831 (1970).

<sup>18</sup>G. H. Parker, T. C. McGill, C. A. Mead, and D. Hoffman, Solid State Electron. **11**, 201 (1968).

<sup>19</sup>S. L. Kurtin, T. C. McGill, and C. A. Mead, Phys. Rev. **B3**, 3368 (1971).

<sup>20</sup>R. H. Fowler and L. W. Nordheim, Proc. Roy. Soc. (Lond.) **A119**, 173 (1928).

<sup>21</sup>M. Lenzlinger and E. H. Snow, J. Appl. Phys. **40**, 278 (1969).

<sup>22</sup>G. H. Parker and C. A. Mead, Phys. Rev. Lett. **21**, 605 (1968).